



Energy, Mines and
Resources Canada

Energie, Mines et
Ressources Canada

CANMET

Canada Centre
for Mineral
and Energy
Technology

Centre canadien
de la technologie
des minéraux
et de l'énergie

PRE-MINING STRESSES AT SOME HARD ROCK MINES IN THE CANADIAN SHIELD

B. ARJANG

ELLIOT LAKE LABORATORY

DECEMBER 1988

Presented at 30th U.S. Symp. on Rock Mechanics, held at West Virginia University, June 19-22, 1989 and published in the Proceedings.

Submitted for publication in CIM Bulletin.

CROWN COPYRIGHT RESERVED

MRL 89-06 (OP, J) c.2.

PRE-MINING STRESSES AT SOME HARD ROCK MINES IN THE CANADIAN SHIELD

B. Arjang, Research Scientist

Elliot Lake Laboratory, CANMET, Energy, Mines and Resources Canada

Elliot Lake, Ontario

ABSTRACT

Ground stresses are one of the significant factors in the context of rockbursts and underground instability at some hard rock mines in Canada. Overcoring strain relief measurements using triaxial strain cells were performed at several mine sites to provide stress data for stability evaluations and mine design. Pre-mining stress determinations carried out at depths between 60 to 1890 m resulted in the following average stress gradients:

Maximum horizontal stress, $\sigma_{Hmax} = 8.18 + 0.0422 \text{ MPa/m depth}$

Minimum horizontal stress, $\sigma_{Hmin} = 3.64 + 0.0276 \text{ MPa/m depth}$

Average horizontal stress, $\sigma_{Ha} = 5.91 + 0.0349 \text{ MPa/m depth}$

Vertical stress, $\sigma_v = 0.0266 \pm 0.008 \text{ MPa/m depth}$

The maximum and minimum horizontal compressive stresses, with an average ratio of 1.75 ± 0.45 , prevail in east-west and northerly directions, respectively. Horizontal compressive stresses in excess of vertical overburden load were determined, indicating large variations in ratios to a depth of about 1000 m with decreasing trend towards depth.

From present data, a particular regional zoning for the magnitude and direction of horizontal stress fields cannot be outlined.

A common feature at mines with near vertical orebodies is that the maximum horizontal stress acts perpendicular to strike while the minimum horizontal stress is aligned on-strike. The vertical stress components approach the gravitational overburden load.

INTRODUCTION

The structural stability of any underground excavation is primarily dependent on the state of pre-mining stress, the stress re-distribution

created by the development of the mine, as well as the in situ strength of the rock material and geological factors. Underground stress measurements in Canadian hard rock mines have been carried out by the Canada Centre for Mineral and Energy Technology (CANMET) since the early 1960's.

As a continuation of the stress determination program, and as part of a Canada/Ontario/Industry rockburst research project, extensive underground stress measurements were conducted in cooperation with operating mining companies. Measurements were taken at depths between 60 to 1890 m in the following mine sites located in Northern Ontario and Quebec: Detour Lake, Selbaie, Montauban, Bousquet, Eldrich, Niobec, Kidd Creek, Dome, Macassa, Stanleigh, and Campbell Red Lake. Overcoring strain relief measurements were made using triaxial strain cells (CSIR and CSIRO). At each site at least two consistent measurements were taken.

The following provides a compilation of several case studies in ground stress determinations (Arjang 1984 to 1988), and an evaluation of selected stress data from 84 overcoring strain relief measurements.

GENERAL GEOLOGICAL-STRUCTURAL SETTING

Most of the ground stress determination sites are located in the Superior Tectonic Province of the Canadian Shield. The characteristic features of the Superior Tectonic Province are the easterly trending, alternating volcanic-plutonic and metasedimentary-gneiss belts, upon which major and minor structures are superimposed. Intense structural deformations of the Archean rock strata occurred during the Kenoran and the subsequent Grenville orogeny.

Available structural data and kinematic analysis derived from the Southern Part of the Superior Tectonic Province suggest a long-standing stress pattern involving north-south horizontal compression and east-west extension

(Goodwin and West 1974). On a local scale, kinematic evidence identified a similar stress field, a major deformation with compression in a NNW-SSE/subhorizontal direction and a subsequent phase of compression in a NE-SW/subhorizontal direction (Herget 1974). Tectonic fabric analysis indicated that this general stress field was active at least up to the Huronian Orogeny (Bielenstein and Eisbacher 1969).

Geological-structural settings at most stress determination sites reflect a complex history of intermittent folding, intrusive activity and faulting or fracturing. The productive gold and base metal sulphide deposits are commonly associated with the felsic volcanic rocks.

RESULTS OF GROUND STRESS DETERMINATIONS

After screening the validity of strain recovery data, the results of the most reliable stress values were compiled and analyzed. Table 1 provides the results of the stress components, the magnitude and direction of the principal compressive stresses in relation to the geographic north, the elastic constants and rock types intersected in the stress determination sites.

Evaluation of stress data indicated that the orientations of the principal compressive stresses were relatively consistent at the stress determination sites. However, some scatter in the orientations occurs within each depth interval and/or different location at the individual mine sites. The scatter of directions was generally greater at shallow depths in highly fractured rock mass. Some variation in the direction of the principal compressive stresses occurs on a regional scale. However, the maximum principal compressive stress prevails horizontal easterly, and the intermediate principal compressive stress a sub-horizontal northerly direction. The minimum principal compressive stress is oriented nearly

vertical. Figure 1 illustrates prevailing directions of the maximum principal compressive stress at each mine in the form of a lower hemisphere of an equal area net projection. The overall orientation of the ore zones is presented on great circles. The spatial distribution of directions of the maximum and the minimum horizontal stresses are presented in Figure 2.

Based on present data, the maximum horizontal stress is on average 1.75 (+0.45) times the minimum horizontal stress. The ratios, ranging from 1.0 to 2.9, indicate significant local as well as regional variations. A nearly isotropic stress field occurs at some locations in the Timmins mining district.

Horizontal stresses in excess of vertical overburden load were determined. The values confirmed previous observations made elsewhere in hard rock mines in the Canadian Shield. The ratio of measured horizontal stress to measured vertical stress, however, varies over a wide range, as follows:

Maximum horizontal/vertical stress = 1.2 to 4.0

Minimum horizontal/vertical stress = 0.7 to 2.0

From present data particular zoning of the horizontal stress fields with respect to the magnitude and direction on a regional scale cannot be outlined.

VARIATION OF VERTICAL AND HORIZONTAL STRESS WITH DEPTH

The following statistical evaluation is based on the results of 64 stress tensor analyses from the selected data obtained at depth from 60 to 1890 m below surface.

Variation of vertical components of the in situ stress with depth is shown in Figure 3. As the data plots indicate, most values of the measured vertical stress follow a straight line with a zero intercept, resulting in an average stress gradient of:

$$\sigma_v = 0.0266 \pm 0.008 \text{ MPa/m}$$

The majority of data (over 80%) fits within a vertical stress gradient range of 0.0202 to 0.0306 MPa/m, when excluding values with deviations greater or less than 40% of the mean gradient of 0.0266 MPa/m obtained from the present data. The increase of the vertical stress component with depth can be related to an average rock density of about 2600 kg/m³ in the area studied.

Variations of horizontal stress magnitudes as a function of depth are shown in Figures 4 and 5. The regression analysis yielded the following stress gradients:

$$\sigma_{Hmax} = 8.18 + 0.0422 \text{ MPa/m} \quad (\text{Correlation coefficient: } 0.91)$$

$$\sigma_{Hmin} = 3.64 + 0.0276 \text{ MPa/m} \quad (\text{Correlation coefficient: } 0.89)$$

Figure 6 shows the variation of the average horizontal stress versus depth. A regression analysis of data resulted in the following relationship:

$$\sigma_{Ha} = 5.91 + 0.0349 \text{ MPa/m} \quad (\text{Correlation coefficient: } 0.91)$$

Recent statistical analysis of the stress data provided an alternative evaluation for the changes of the average horizontal stress with depth in the Canadian Shield (Herget 1986) in the form:

$$0-800 \text{ m: } \sigma_{Ha} = 0.0581 \text{ MPa/m}$$

$$800-2200 \text{ m: } \sigma_{Ha} = 35.79 + 0.0111 \text{ MPa/m}$$

The above functions suggest that no uniform stress gradients between 0-2200 m exist and the evaluated data fit within two straight-line relationships with a break at 800 m. As illustrated in Figure 6, a comparison shows that differences between the two sets of data are not significant.

The ratios of the maximum, minimum and average horizontal stresses to vertical stress show large dispersion at depths of less than about 1000 m. For depths greater than 1000 m, however, stress ratios indicate a decreasing trend towards depth.

APPLICATION OF GROUND STRESS DATA FOR STABILITY EVALUATION

Before ground stress measurements became a routine process in the Canadian deep hard rock mines, the estimated gravitational overburden load was considered as the only stress factor for mine design and stability evaluations. Stress determination results, however, suggest anisotropic horizontal compressive stresses in excess of the vertical stress component. Regarding the complex stress field, for numerical modelling of mining excavations it is, therefore, required to input the vertical stress gradient and the horizontal stresses as a ratio of the vertical stress. The horizontal to vertical stress ratios perpendicular to strike and on-strike of the orebody for individual mine sites are listed in Table 2.

The results indicate that a common feature at mines with near vertical orebodies is that the maximum horizontal stress acts perpendicular to strike and the minimum horizontal stress is aligned on-strike.

CONCLUSIONS

The present data suggest that a pervasive homogeneous stress field does not exist in the Canadian Shield. Local stress fields are affected by geological-structural conditions and changes in the physical rock properties. The stress regime, however, on a regional scale indicates common features regarding direction of the horizontal stresses, magnitudes of the vertical stress components and ratios of the horizontal to vertical stress.

The average pre-mining stress gradients produced essential information for the stability evaluations of rockburst-prone hardrock mines as well as mines at an early stage of development.

As variations in the state of stress exist, only initial estimates of ground stresses can be made from the present data for regional stability

assessments in the Canadian hardrock mines. Therefore, determination of ground stresses as input parameters for numerical modelling of mining excavations still remains essential at the individual mine sites. Field observations suggest that measurements at different locations are required in order to extrapolate the stress data to a larger scale of the mine.

ACKNOWLEDGEMENTS

The projects on ground stress determination could only be accomplished by the active participation and support of the following mining companies: Campbell Red Lake Mines Ltd., Cambior Inc., Dome Mines Ltd., Kidd Creek Mines Ltd., Lac Minerals Ltd., Les Services TMG Inc., Rio Algom Ltd., Selnor Inc. and Muscocho Exploration Ltd.

REFERENCES

- Arjang, B., 1984-1988 Division Reports, MRP/MRL 84-55(TR); MRP/MRL 84-119(TR); MRP/MRL 85-63(TR); MRP/MRL 85-67(TR); MRL 87-15(TR); MRL 87-108(TR); MRL 87-142(TR); MRL 87-147(TR); MRL 88-59(TR); MRL 88-87(TR); MRL 88-93(TR); MRL 88-132(TR). CANMET, Energy, Mines and Resources Canada.
- Bielenstein, H.U. and G.H. Eisbacher 1969. Tectonic interpretation of elastic strain-recovery measurements at Elliot Lake, Ontario. Research Report R210, CANMET, Energy Mines and Resources Canada.
- Goodwin, A.M. and G.F. West, 1974. The superior geotraverse project. Geoscience Canada, vol. 1, pp. 21-29.
- Herget, G. 1974. Ground stress determinations in Canada. Rock Mechanics vol. 6, pp 53-64.
- Herget, G. and P. Miles 1976. Underground stress determinations using the doorstopper method at Timmins, Ontario. Division Report MRP/MRL 76-148(TR), CANMET, Energy, Mines and Resources Canada.

Herget, G. 1976. Field testing of modified triaxial strain cell equipment at Timmins, Ontario. Division Report MRP/MRL 77-2(TR), CANMET, Energy, Mines and Resources Canada.

Herget, G. 1986. Changes of ground stresses with depth in the Canadian Shield. Proceedings International Symposium on Rock Stress and Rock Stress Measurements, pp 61-68, Stockholm, Sweden.

Quesnel, W.J. 1985. In situ stress measurements, No. 2 mine, 36-6 sub-level. Ground control Section, Kidd Creek Mine.

Table 1 - Results of field stress determinations (stress in MPa).

Depth (m)	σ_{EW}	σ_{NS}	Stress Components			τ_{VE}	* %	Principal σ_1 Brg./Dip	Compressive σ_2 Brg./Dip	Stress σ_3 Brg./Dip	E (GPa)	ν	Rock Type
			σ_V	τ_{EN}	τ_{NV}								
<u>Detour Lake Mine</u>													
60	3.0	2.1	1.5	0.3	0.3	1.5	33	4.0 257/32	2.0 348/02	0.6 082/58	65.7	0.24	Basalt
<u>Selbaie Mine</u>													
70	1.0	2.0	1.6	-1.7	-0.3	0.6	10	3.4 165/19	1.4 015/68	0.5 258/10	62.8	0.21	Dacite
180	6.6	3.4	2.0	-0.7	0.2	-0.9	4	6.9 312/10	3.3 034/01	1.8 128/80	69.7	0.25	Dacite
180	11.3	4.7	2.1	-1.6	0.04	-0.7	45	11.7 304/04	4.3 214/03	2.0 090/85	69.7	0.25	Dacite
180	11.1	7.2	6.6	-1.6	-0.2	0.2	4	11.7 132/03	6.8 227/56	6.6 040/34	69.7	0.25	Dacite
290	13.3	7.5	6.4	-2.6	0.0	-1.9	2	14.7 312/12	6.9 213/35	5.6 238/52	64.9	0.29	Dacite
<u>Montauban Mine</u>													
81	3.1	8.1	4.0	1.1	-2.8	-1.5	38	10.0 015/28	3.4 124/31	1.8 252/46	53.1	0.17	Gneiss
81	4.3	9.5	3.7	5.5	-2.9	-1.7	6	14.1 032/18	2.6 223/72	0.8 123/03	50.7	0.25	Gneiss
81	5.5	7.9	2.6	-2.0	2.5	0.6	22	9.6 157/17	5.2 255/25	1.2 037/59	50.7	0.25	Gneiss
124	7.1	11.3	4.2	-0.5	3.3	-0.4	2	12.6 174/21	7.0 083/01	3.0 352/69	25.6	0.20	Gneiss
<u>Bousquet Mine</u>													
190	9.2	11.9	5.0	3.4	-1.1	-0.2	20	14.6 034/06	7.0 303/12	4.8 152/76	47.0	0.29	Tuff
190	15.8	17.5	7.4	2.3	0.7	-1.2	5	19.1 035/00	14.4 125/11	7.2 303/79	47.0	0.29	Tuff
900	41.2	45.8	17.7	7.8	-7.3	-14.4	13	57.2 044/21	36.8 138/11	10.5 256/66	66.9	0.24	Tuff
900	44.0	43.5	19.1	8.0	0.3	-1.1	8	51.8 046/00	35.8 136/03	19.0 300/86	53.1	0.21	Tuff
<u>Eldrich Mine</u>													
115	11.4	5.2	3.1	0.6	-2.5	-2.4	35	12.3 079/18	6.3 340/26	1.2 200/58	69.0	0.23	Tonalite
115	8.9	6.4	3.5	-1.2	-0.9	0.3	26	9.4 294/06	6.1 025/15	3.3 184/74	69.0	0.23	Tonalite
276	20.6	9.0	7.4	-0.8	-1.0	4.7	28	22.2 275/18	9.0 009/11	5.7 129/69	69.0	0.23	Tonalite
276	17.4	10.2	5.8	4.1	-4.4	0.02	31	19.6 062/08	11.1 326/35	2.7 164/54	69.0	0.23	Tonalite
<u>Niobec Mine</u>													
260	21.0	16.5	13.8	3.0	-0.2	-1.3	26	22.7 064/08	15.1 156/15	13.5 308/73	74.6	0.26	Carbonatite
260	22.9	16.9	7.3	5.2	0.9	-6.7	30	27.7 064/15	15.7 160/21	4.3 301/64	74.6	0.26	Carbonatite
260	11.0	9.7	10.8	-1.6	-1.3	-0.3	7	12.3 314/24	11.1 083/54	8.1 212/24	74.6	0.26	Carbonatite
260	10.0	16.7	5.5	8.2	-3.2	-1.5	10	23.0 214/11	5.2 110/50	4.1 312/37	74.6	0.26	Carbonatite
305	19.4	8.2	7.3	-2.3	-0.5	0.2	6	19.9 101/02	8.0 192/32	7.0 009/58	74.8	0.35	Carbonatite
305	22.2	7.2	9.4	-0.1	0.02	1.1	3	22.3 090/05	9.4 180/01	7.2 280/85	74.8	0.35	Carbonatite
<u>Kidd Creek Mine</u>													
488**	31.9	25.4	13.4	2.8	5.0	-3.6	12	33.2 094/06	26.8 186/23	10.7 350/66	95.8	0.27	Andesite
732	28.0	32.7	18.7	5.4	-3.5	12.7	22	38.3 258/25	32.8 002/27	8.4 133/52	65.0	0.31	Rhyolite
732	54.2	33.9	22.2	5.2	-5.1	-11.3	7	59.5 095/18	33.0 002/08	17.9 261/70	65.0	0.31	Rhyolite
853**	51.0	52.5	20.9	0.8	-0.2	7.4	16	53.3 250/10	51.9 342/09	19.1 112/77	95.8	0.27	Andesite
853**	61.6	50.1	34.6	5.1	7.7	14.8	12	67.9 086/16	48.6 355/10	28.1 236/72	95.6	0.30	Andesite
853**	44.8	42.9	23.6	7.1	-1.1	14.7	2	53.2 077/12	39.9 170/18	16.3 318/70	77.6	0.27	Andesite
1041*	39.7	50.1	34.4	-7.0	-4.3	2.2	23	54.8 353/13	36.2 263/01	33.2 170/77	96.5	0.29	Andesite
1382	60.8	28.3	37.6	-9.0	5.2	13.3	5	69.4 126/24	31.7 271/62	25.5 029/14	87.9	0.22	Andesite
1382	68.5	41.6	33.0	8.6	-8.8	-9.0	11	74.1 091/16	41.8 354/24	27.2 211/61	87.9	0.22	Andesite

Depth (m)	Stress Components							* %	Principal Compressive Stress			E (GPa)	ν	Rock Type
	σ _{EW}	σ _{NS}	σ _V	TEN	TNV	TVE	σ ₁ Brg./Dip		σ ₂ Brg./Dip	σ ₃ Brg./Dip				
<u>Dome Mine</u>														
438	15.8	14.3	12.3	1.0	3.9	0.7	4	18.0	15.1	9.2	59.8	0.24	Porphyry	
								215/32	113/18	358/52				
438	19.0	14.3	12.4	-1.3	5.8	1.8	20	19.5	19.1	7.0	59.8	0.24	Porphyry	
								249/28	143/28	016/48				
937	38.2	26.4	27.2	8.4	2.2	-1.6	2	42.6	28.4	20.9	63.3	0.28	'Greenstone'	
								063/02	157/67	332/23				
937	30.0	24.6	29.5	8.0	7.6	4.7	5	45.5	28.5	18.2	63.3	0.28	'Greenstone'	
								239/26	114/49	345/28				
1238	53.3	33.9	25.3	-1.1	3.8	0.6	3	53.3	35.3	23.8	65.6	0.29	'Greenstone'	
								273/01	183/21	005/69				
1238	50.9	42.9	28.2	2.9	3.8	2.3	1	52.0	42.5	27.2	65.6	0.29	'Greenstone'	
								249/08	158/10	017/77				
<u>Macassa Mine</u>														
1585	40.4	64.2	38.9	-6.6	5.0	-6.8	11	67.5	43.2	32.8	64.3	0.16	Syenite	
								343/13	062/40	088/47				
1585	53.1	46.3	31.8	-7.8	6.4	-8.9	1	62.2	41.2	27.7	64.3	0.16	Syenite	
								304/20	395/02	131/70				
1585	33.7	52.8	30.3	0.5	4.5	-3.0	18	54.1	33.6	29.2	64.3	0.16	Syenite	
								168/10	261/16	046/71				
1890	61.0	80.7	50.8	0.4	9.0	-3.3	1	83.2	61.8	47.5	68.6	0.19	Syenite	
								359/16	265/13	138/70				
1890	39.3	66.1	35.2	13.1	13.9	1.7	7	76.0	36.1	28.5	68.6	0.19	Syenite	
								021/18	280/30	137/54				
1890	67.8	79.7	48.4	3.7	17.9	1.2	3	88.6	67.1	40.2	68.6	0.19	Syenite	
								012/24	280/05	178/66				
<u>Stanleigh Mine</u>														
1066	28.6	31.9	28.2	-0.4	-3.6	-2.1	1	34.2	29.6	25.0	75.5	0.17	Quartzite	
								196/33	300/20	056/50				
1066	57.5	39.7	21.5	9.2	-4.5	-6.9	1	62.9	35.9	19.8	75.5	0.17	Quartzite	
								253/11	162/05	048/78				
<u>Campbell Red Lake Mine</u>														
580	25.6	11.9	8.2	2.5	-7.1	-0.1	12	26.2	16.9	2.6	74.3	0.25	Andesite (altered)	
								078/05	344/38	174/52				
580	29.7	16.6	8.3	3.3	-6.0	-1.4	3	30.8	18.6	5.1	74.3	0.25	Andesite (altered)	
								074/08	340/26	179/62				
625	9.2	21.4	9.7	3.9	3.3	-0.04	41	23.2	9.5	7.5	91.7	0.21	Andesite	
								195/13	086/55	293/31				
625	17.3	14.6	14.5	2.6	0.5	-5.7	4	22.2	15.0	9.2	91.7	0.21	Andesite	
								074/35	183/25	300/45				
625	22.5	16.5	10.8	3.1	-1.6	0.3	10	23.8	15.7	10.2	91.7	0.21	Andesite	
								067/02	336/18	162/72				
625	20.3	28.6	19.4	14.3	4.6	3.2	35	40.8	17.9	9.5	90.5	0.23	Andesite	
								217/15	042/75	307/01				
625	18.1	20.6	11.3	-3.6	1.5	-3.5	52	24.0	16.1	9.8	90.5	0.23	Andesite	
								141/15	046/17	270/67				
625	17.9	8.2	19.5	7.0	-4.4	-1.8	-	24.5	17.2	3.9	86.5	0.21	Andesite	
								056/38	258/49	155/11				
670	42.9	39.9	26.5	-13.5	-15.1	7.6	5	62.2	30.6	16.6	83.5	0.20	Andesite	
								317/24	058/23	185/55				
670	47.6	5.5	20.9	-4.8	-7.0	6.4	23	49.9	21.3	2.6	83.5	0.20	Andesite	
								278/14	042/65	183/20				
670	41.1	17.5	18.1	0.8	7.5	-3.7	12	41.7	25.0	10.0	83.5	0.20	Andesite	
								091/09	190/44	352/44				
990	41.8	28.6	16.5	9.7	-10.0	-5.5	3	49.8	26.2	10.9	85.3	0.22	Andesite	
								058/17	321/23	180/61				
990	40.7	18.4	17.5	1.4	-1.7	-4.2	5	41.6	19.0	15.3	85.3	0.22	Andesite	
								086/10	351/26	195/62				
990	61.8	18.7	20.9	5.7	-11.6	-15.4	3	68.6	25.5	7.2	85.3	0.22	Andesite	
								079/20	333/37	195/47				
1220	78.0	37.2	21.2	12.6	-10.9	4.5	30	81.6	40.7	14.1	84.8	0.20	Andesite	
								254/01	345/31	162/59				
1220	55.9	43.1	37.9	8.5	4.5	14.2	N/A	67.4	39.3	30.1	84.8	0.20	Andesite	
								246/27	341/11	092/61				
1220	56.7	49.7	43.7	9.9	7.5	16.2	N/A	74.1	43.5	32.6	84.8	0.20	Andesite	
								238/30	336/12	085/57				

*Average standard error for the stress components (in percent).

σ₁, σ₂, σ₃: Principal compressive stresses, directions (Bearing/Dip) in degrees from the geographic north.
E: Elastic modulus. ν: Poisson's ratio. ** (Herget et al. 1976, Herget 1976), *(Quesnel 1985).

Table 2 - Pre-mining horizontal/vertical stress ratios
in relation to the orebody.

Mine Site	Depth (m)	Orebody (Overall trend)	Stress Ratios*		
			$\frac{\sigma_{Ha}}{\sigma_V}$	$\frac{\sigma_{H\perp}}{\sigma_V}$	$\frac{\sigma_{H\parallel}}{\sigma_V}$
Detour Lake	60	E-W/vert.	2.0	1.3	2.6
Selbaie	70	NNE-SSW/sub-vert.	1.5	2.1	0.9
	180	"	2.6 \pm 1.2	3.6 \pm 1.8	1.6 \pm 0.5
	290	"	1.7	2.3	1.1
Montauban	81	NW-SE/horiz.	2.3 \pm 0.6	3.3 \pm 0.7	1.2 \pm 0.7
	124	"	3.1	3.5	2.7
Bousquet	190	ESE-WNW/vert.	2.2 \pm 0.1	2.7 \pm 0.1	1.7 \pm 0.3
	900	"	2.5 \pm 0.2	2.9 \pm 0.3	1.9 \pm 0.1
Eldrich	115	NNE-SSW/sub-vert.	2.6 \pm 0.5	3.3 \pm 0.8	1.9 \pm 0.2
	276	"	2.3 \pm 0.3	3.2 \pm 0.2	1.5 \pm 0.5
Niobec	260	NNE-SSW/vert.	2.0 \pm 0.9	2.7 \pm 1.5	1.3 \pm 0.6
	305	"	1.8 \pm 0.1	2.5 \pm 0.2	1.0 \pm 0.1
Kidd Creek	488	NNW-SSE/vert.	2.2	2.5	2.0
	732	"	2.0 \pm 0.1	2.3 \pm 0.4	1.6 \pm 0.1
	853	"	2.1 \pm 0.4	2.2 \pm 0.2	1.9 \pm 0.6
	1041	"	1.7	2.0	1.3
	1382	"	1.5 \pm 0.2	2.0 \pm 0.2	1.0 \pm 0.3
Dome	438	ENE-WSW/sub-vert.	1.4 \pm 0.2	1.3 \pm 0.2	1.5 \pm 0.1
	937	"	1.2 \pm 0.1	1.0 \pm 0.0	1.6 \pm 0.0
	1238	"	1.7 \pm 0.0	1.4 \pm 0.1	1.9 \pm 0.2
Stanleigh	1066	ESE-WNW/horiz.	1.7 \pm 0.8	1.4 \pm 0.4	2.0 \pm 1.2
Campbell Red Lake	580	NW-SE/vert.	2.8 \pm 0.2	3.4 \pm 0.3	2.1 \pm 0.1
	625	"	1.5 \pm 0.3	1.9 \pm 0.4	1.1 \pm 0.2
	670	"	1.7 \pm 0.0	2.3 \pm 0.0	1.2 \pm 0.2
	990	"	2.0 \pm 0.3	2.9 \pm 0.4	1.3 \pm 0.2
	1220	"	1.9 \pm 0.8	2.5 \pm 1.2	1.3 \pm 0.5
Macassa	1585	NE-SW/vert.	1.5 \pm 0.1	1.8 \pm 0.1	1.2 \pm 0.1
	1890	"	1.5 \pm 0.1	1.8 \pm 0.1	1.2 \pm 0.2

*Range of horizontal/vertical stress: average ($\frac{\sigma_{Ha}}{\sigma_V}$), perpendicular ($\frac{\sigma_{H\perp}}{\sigma_V}$), and parallel ($\frac{\sigma_{H\parallel}}{\sigma_V}$) to the prevailing trend of the orebody.

FIGURES

Fig. 1 - Stress determination sites and the direction of maximum principal compressive stress in the Canadian Shield.

Fig. 2 - Direction frequency plots of maximum and minimum horizontal compressive stresses.

Fig. 3 - Variation of vertical stress components with depth.

Fig. 4 - Variation of maximum horizontal compressive stress with depth.

Fig. 5 - Variation of minimum horizontal compressive stress with depth.

Fig. 6 - Variation of average horizontal compressive stress with depth.

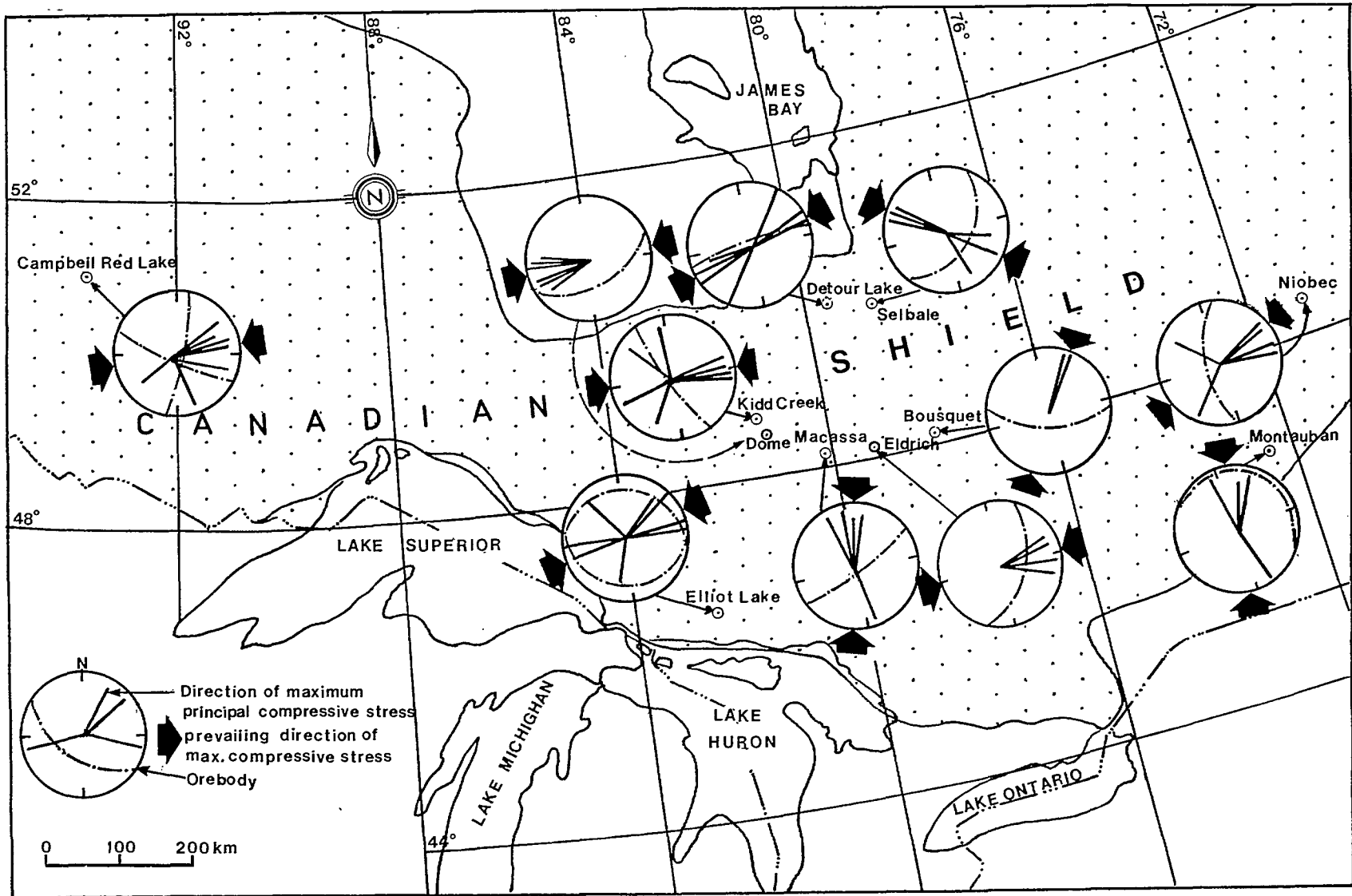


Figure 1

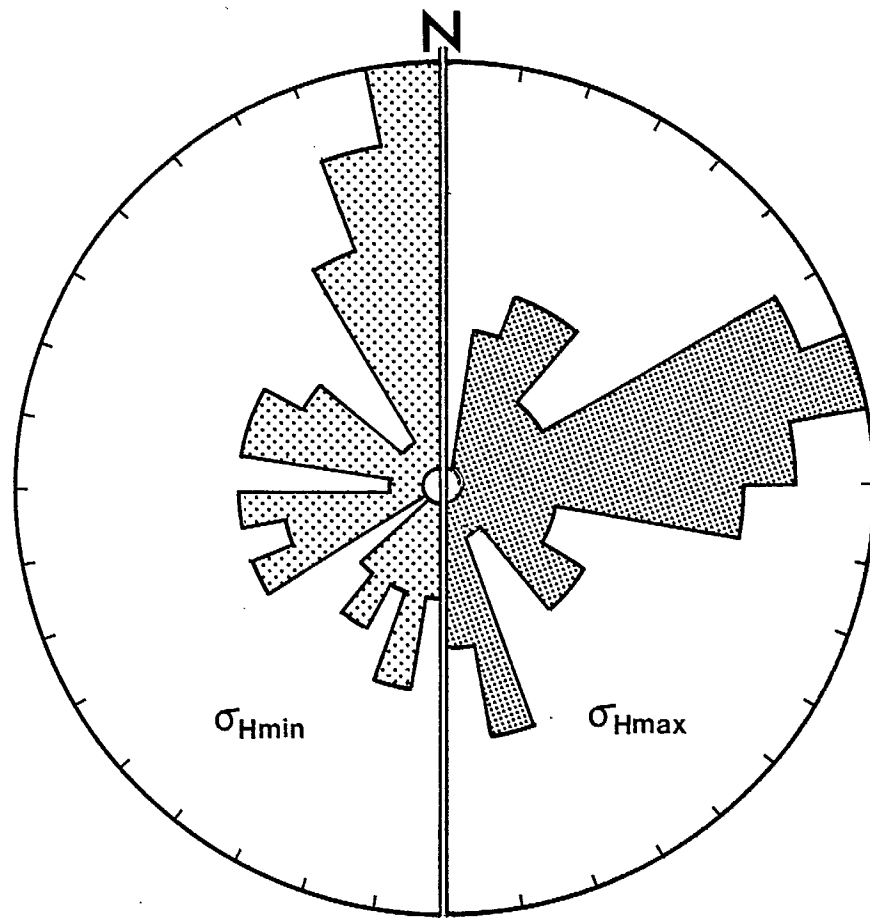


Figure 2

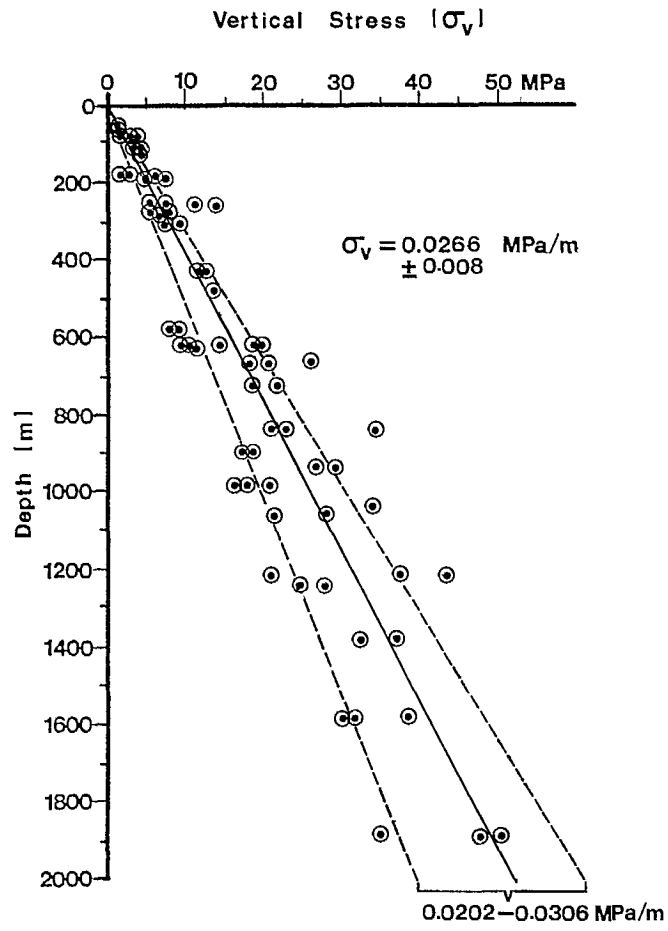


Figure 3

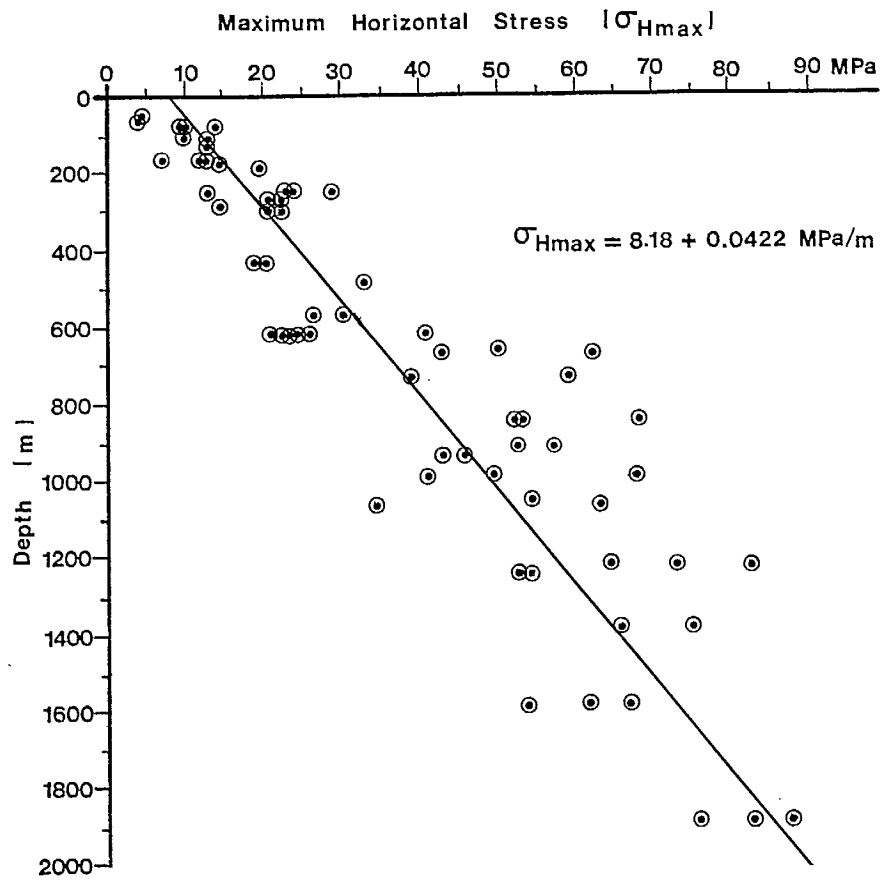


Figure 4

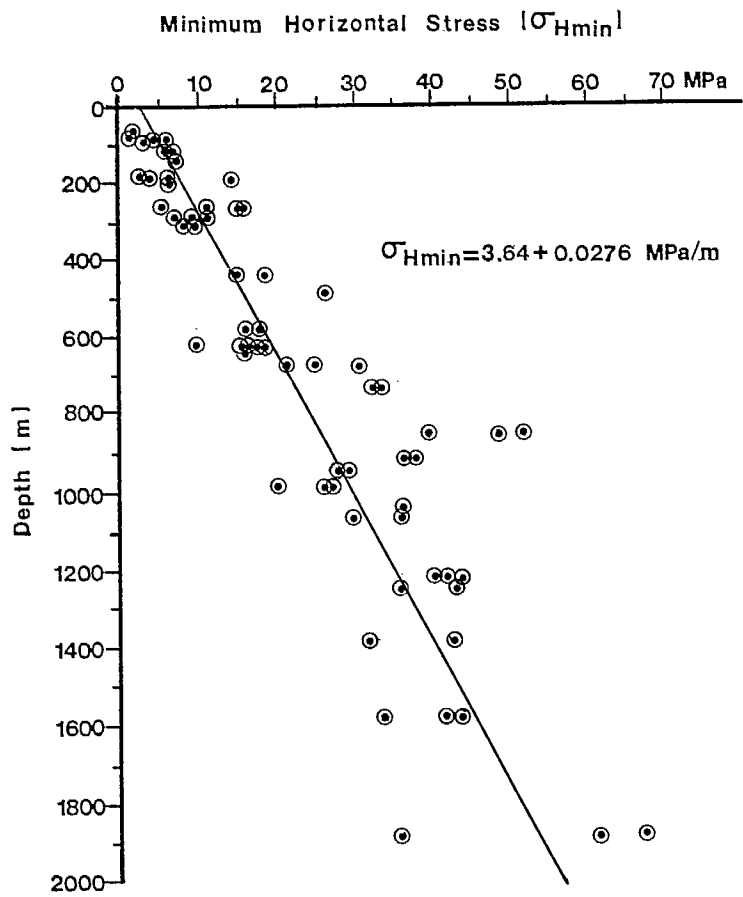


Figure 5

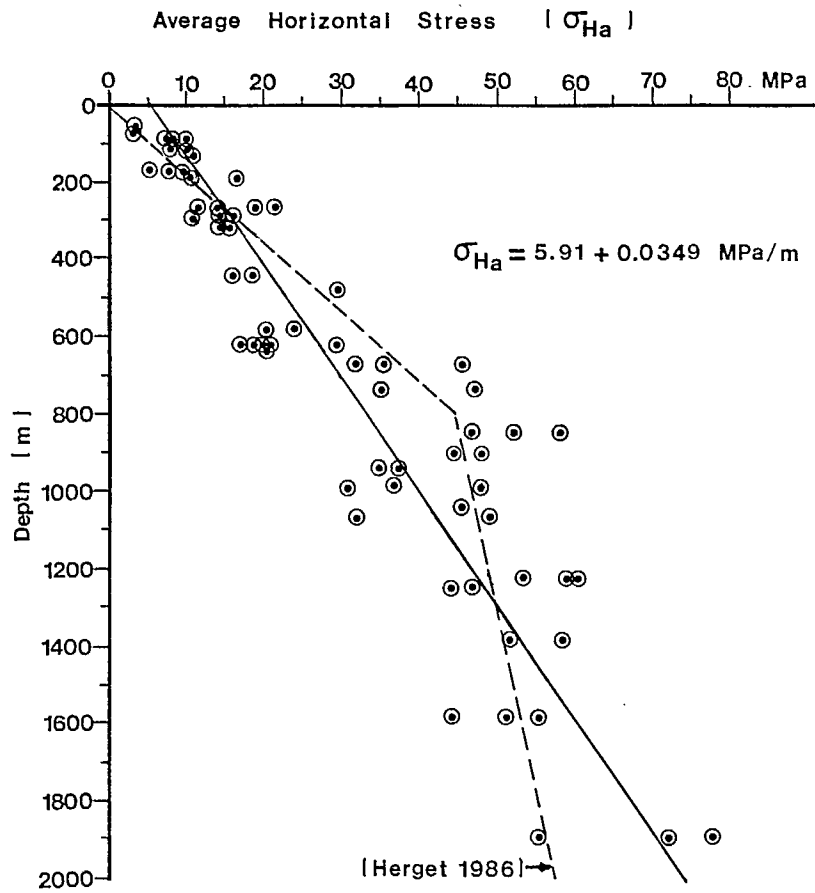


Figure 6